

Friction and wear properties of C/C–SiC braking composites

Xuan Zhou^{*}, Dongmei Zhu, Qiao Xie, Fa Luo, Wancheng Zhou

State Key Laboratory of Solidification Processing, Northwestern Polytechnical University, Xi'an 710072, China

Received 14 October 2011; accepted 6 November 2011

Available online 11 November 2011

Abstract

Two series of C/C–SiC composites were fabricated via precursor infiltration pyrolysis (PIP) and chemical vapor infiltration (CVI) using porous C/C composites with different original densities as preforms, respectively. The tribological characteristics of C/C–SiC braking composites were investigated by means of MM-1000 type of friction testing machine. The friction and wear behaviors of the two series of composites were compared and the factors that influence the friction and wear properties of C/C–SiC composites were discussed. Results show that the friction and wear properties relate close-knit to the content of SiC and porosity. As the original preform density increasing, the content of SiC and porosity decrease, and then the friction coefficient increases obviously, the braking time and the wear rate both decrease. Preparation techniques play an important role in the tribological properties of C/C–SiC composites. Compared with PIP process, the samples from CVI have a little higher friction coefficient, shorter braking time and higher wear rate.

© 2011 Elsevier Ltd and Techna Group S.r.l. All rights reserved.

Keywords: B. Porosity; C/C–SiC composites; PIP; CVI; Friction and wear properties

1. Introduction

The potential for using C/C materials in brake discs and pads has been known for fairly a long time [1]. Because of their outstanding properties, such as low density, excellent strength up to high temperatures, low coefficient of thermal expansion, C/C frictional components were applied in aircraft, racing cars and motorcycles [2–5]. However, C/C brakes suffer from high wear rate and poor oxidation resistance, which restrict its application seriously [6,7].

C/C–SiC composites, the carbon fiber reinforced dual matrices composites, introducing SiC in C/C, exhibit high and stable friction coefficients, low wear rates, high thermal shock resistance, and preferable oxidation resistance in comparison with traditional brake materials [8–10]. Nowadays, C/C–SiC composites have been demonstrated to be the top choice as the advanced brake systems.

At present, C/C–SiC can be fabricated by various methods including chemical vapor infiltration (CVI), precursor

infiltration pyrolysis (PIP), liquid silicon infiltration (LSI) and so on [11,12]. Each of the above routes displays both advantages and drawbacks. CVI and PIP are both slow densification technique and yield materials with some residual porosity. The materials fabricated by LSI often contain free silicon, which seriously affects their frictional properties [13]. And the composites from LSI display relatively poor mechanical properties [12].

In this study, two series of C/C–SiC composites were fabricated via different methods, including PIP and CVI, respectively. The friction and wear properties of C/C–SiC composites from different techniques were compared and the effects of porosity and SiC contents on the tribological properties of C/C–SiC composites were discussed.

2. Experimental

2.1. Manufacture of the composites

The C/C preforms with different original densities were produced by chemical vapor deposition process (CVD) firstly and then the C/C–SiC samples were developed via the following two methods including PIP and CVI, respectively.

^{*} Corresponding author. Tel.: +86 29 88494574; fax: +86 29 88494574.

E-mail addresses: 271917028@qq.com (X. Zhou),
dzhunwpu@nwpu.edu.cn (D. Zhu).

2.1.1. PIP

The preceramic polymer was polycarbosilane (PCS). At first, the preforms were infiltrated in a 50 wt.% PCS-xylene solution in vacuum. The preforms filled with precursor were then pyrolyzed in an inner atmosphere at 1600 °C for 2 h. In order to densify the composites, the infiltration-pyrolysis processes were repeated until the weight increments were less than 0.5%. Three group samples, the original densities of which were 1.03 g/cm³, 1.23 g/cm³ and 1.47 g/cm³, marked as Groups 1–3, were obtained via the PIP method. The detailed parameters of the obtained composites are shown in Table 1.

2.1.2. CVI

The SiC CVI was performed using a mixture of methyl-trichloro-silane (MTS, CH₃SiCl₃) and hydrogen. MTS was used as precursor in this study, which was carried by argon. And hydrogen was used as a dilute gas to slow the reaction rate. After deposition, the surfaces of the samples were ground about 1 mm to protect the pores from covering. The process described above was repeated until the weight increments were less than 0.5%. Three group samples, the original densities of which were 1.15 g/cm³, 1.23 g/cm³ and 1.44 g/cm³, marked as Groups 4–6, were obtained via the CVI method. The detailed parameters of them are shown in Table 2.

2.2. Characterization

Friction and wear tests were carried out on a MM-1000 friction testing machine with C/C–SiC composites as both rotating discs and corresponding stationary discs (Fig. 1). The tests would not stop until the friction coefficient was not sensitive to brake times. The testing conditions were as follows: the rotational speed 7500 rpm, the running inertia 2.6 kg m s²,

and the braking pressure 0.82 MPa. Prior to the tests, the surface of specimens and the counterparts were rubbed against each other many times to reach 80% of tangent area. At the end of tests, the linear wear was measured using a micrometer callipers with the precision of 0.01 mm.

The brake torque was obtained from the simulating system directly, and the average friction coefficient can be calculated by the following equation:

$$\mu = \frac{M}{P \cdot S \cdot r}$$

where M is the brake torque, P is the brake specific pressure, S is the frictional area when braking (22.8 cm²), r is the average friction radius (3.3 cm).

The worn tracks of the samples were observed by a JSM-64600 SEM. The densities of samples were measured by Archimedeian method, from which the interrelated fractional open porosity can be calculated. The weight increment of samples was reckoned to be the content of SiC.

3. Results and discussion

3.1. Density, SiC content, and porosity

The density, SiC content, and porosity of samples from different methods are shown in Tables 1 and 2. Despite of different original preform densities, the final densities of samples are of little difference. For the samples with similar original density from different method, the final densities are almost the same. All the brake pairs are with approximate final densities, which could cooperate to work in this study.

It can also be seen that both the SiC content and porosity decrease obviously with the increase of the original densities, as

Table 1
Density, SiC content, and porosity of samples from PIP.

Group		Original density (g/cm ³)	Final density (g/cm ³)	SiC content (%)	Porosity (%)
1	Rotating disc	1.03	1.883	45.20	15.08
	Stationary disc	1.03	1.886	42.43	14.99
2	Rotating disc	1.23	1.897	35.17	8.64
	Stationary disc	1.23	1.902	38.10	7.64
3	Rotating disc	1.47	1.892	22.31	1.81
	Stationary disc	1.47	1.897	22.50	1.68

Table 2
Density, SiC content, and porosity of samples from CVI.

Group		Original density (g/cm ³)	Final density (g/cm ³)	SiC content (%)	Porosity (%)
4	Rotating disc	1.15	1.921	41.45	13.59
	Stationary disc	1.15	1.916	44.91	13.72
5	Rotating disc	1.23	1.885	39.03	10.89
	Stationary disc	1.23	1.848	40.43	12.38
6	Rotating disc	1.44	1.886	24.80	3.15
	Stationary disc	1.44	1.865	23.59	3.71

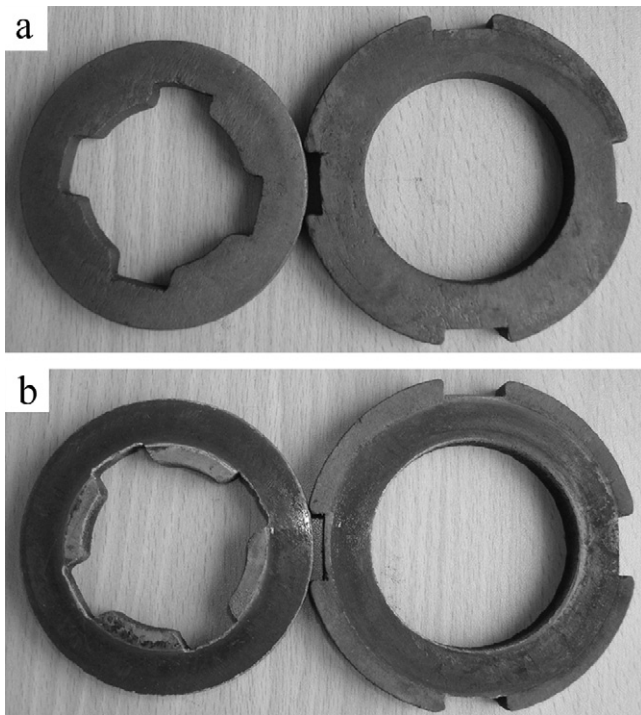


Fig. 1. Photos of a typical C/C–SiC friction discs before and after braking test (a, before test; b, after test).

shown in Figs. 2 and 3. For Groups 3 and 6, the porosity is the best while the SiC content are lowest.

3.2. The friction coefficient and braking time

The friction and wear results of different samples prepared by PIP and CVI are shown in Tables 3 and 4. From Table 3, it is obvious that the friction coefficient of Group 3 is the largest, the braking time the shortest, and the linear wear the smallest, indicating that the friction and wear properties of Group 3 are

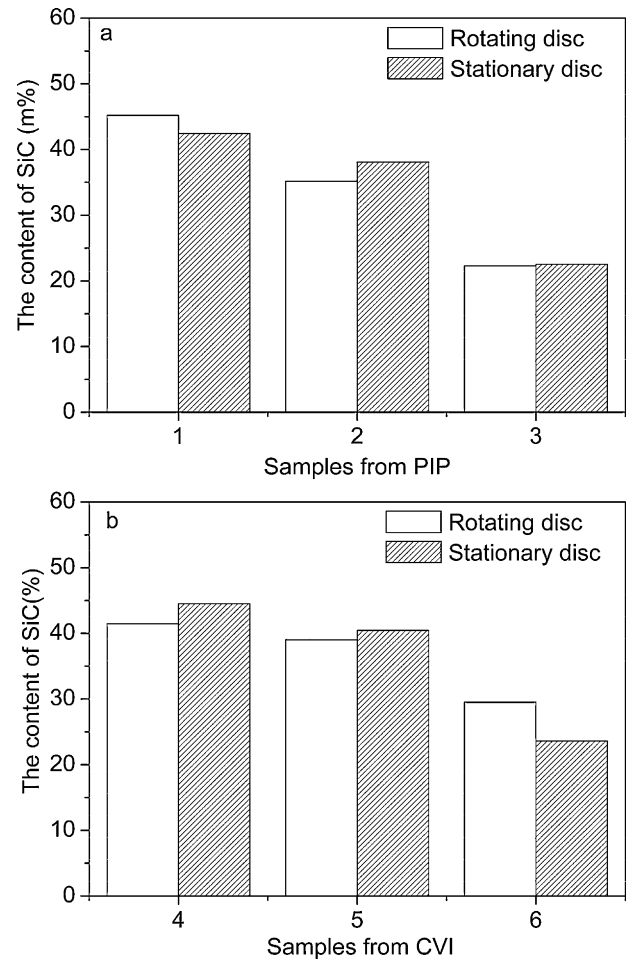


Fig. 2. SiC content of samples from different methods (a, PIP; b, CVI).

the best among the samples from PIP. For the samples from CVI, Group 6 exhibits the best friction and wear properties.

The friction coefficient curves of samples from different methods are shown in Fig. 4. It can be seen that both the friction

Table 3
Friction and wear properties of samples from PIP.

Group	1	2	3
Average friction coefficient	0.2363	0.2487	0.3144
Average torque (N m)	14.17	14.94	18.97
Stability of curve	0.4092	0.3976	0.4983
Absorbing power per unit area (W/cm ²)	243.9	258.9	324.1
Braking time (s)	14.19	13.02	9.54
Wear (rotating/stationary) (mm/time)	0.0015/0.0015	0.0016/0.0014	0.0006/0.0006

Table 4
Friction and wear properties of samples from CVI.

Group	4	5	6
Average friction coefficient	0.2857	0.3114	0.3575
Average torque (N m)	17.02	19.03	21.45
Stability of curve	0.4790	0.4543	0.5220
Absorbing power per unit area (W/cm ²)	294.5	316.3	375.5
Braking time (s)	11.93	11.12	9.38
Wear (rotating/stationary) (mm/time)	0.0063/0.0017	0.0068/0.0033	0.0013/0.0010

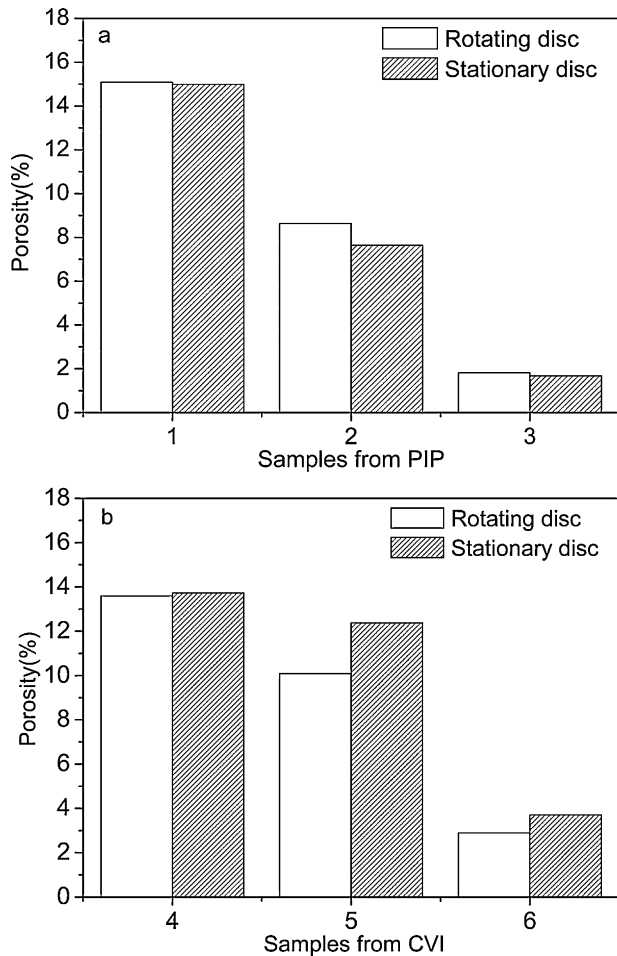


Fig. 3. Porosity of samples from different methods (a, PIP; b, CVI).

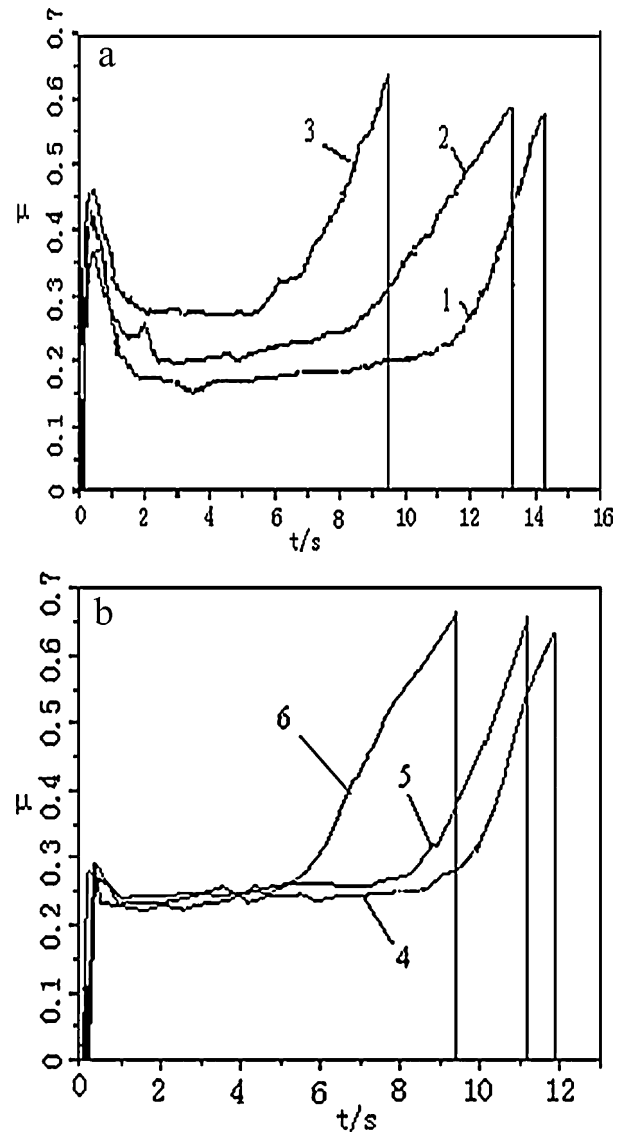


Fig. 4. Curves of friction coefficient for samples from different methods (a, PIP; b, CVI).

coefficient curves are fluctuant and there is a so-called “first peak” in the beginning period of braking. When the braking starts, the surface pressure of brake pairs will increase suddenly, the grains of samples surface will embed mutually and generate new abrasive particles, leading to the rapid increase of friction. Some of the abrasive particles are then pulverized as a layer of frictional film, which plays a role of lubricant, and the friction coefficient may reduce. When the lubrication balances the abrasive friction, the curves tend to change smoothly, as shown in the intermediate section of curves. At the end of braking, due to the inherent peculiarity of the composites, such as the structural flaw, high surface energy and so on, the high temperature caused by friction may lead to the decomposition of the material and then the friction coefficient starts to increase, which takes on the so-called “rise of the tail” phenomenon in the friction coefficient curves.

It can also be found from the friction coefficient curves that the “first peak” phenomenon appeared in PIP is more intense than that in CVI. Because the shrinkage caused by pyrolysis engenders the crack of matrix in PIP process, the surface of samples from PIP is rougher than that from CVI.

The dependence of average friction coefficient and moment of samples from different methods on the original density are shown in Fig. 5. It can be seen that the average friction torque

and friction coefficient increase significantly with the increase of original density, which could be attributed to the difference of SiC content and porosity.

As is well-known, SiC is characterized as high rigidity, abrasion resistance, corrosion resistance, high thermal conductivity, high intensity, having a strong influence on the tribological properties of samples. On the one hand, the rigid SiC works as a framework in the samples to enhance the friction and fix the abrasive particles in the process of friction. On the other hand, as a abrasive, SiC plays a lubricant role when the content of SiC is too high [9,14], which will reduce the friction coefficient. Meanwhile, high porosity may stunt the forming of SiC framework and spur the forming of abrasive film, which will deteriorate the tribological properties. For samples with low original density in this study, higher SiC content and porosity may trend to lower the friction coefficient, no matter what method the samples are from. Consequently, Groups 1 and 4 exhibit the worst friction properties.

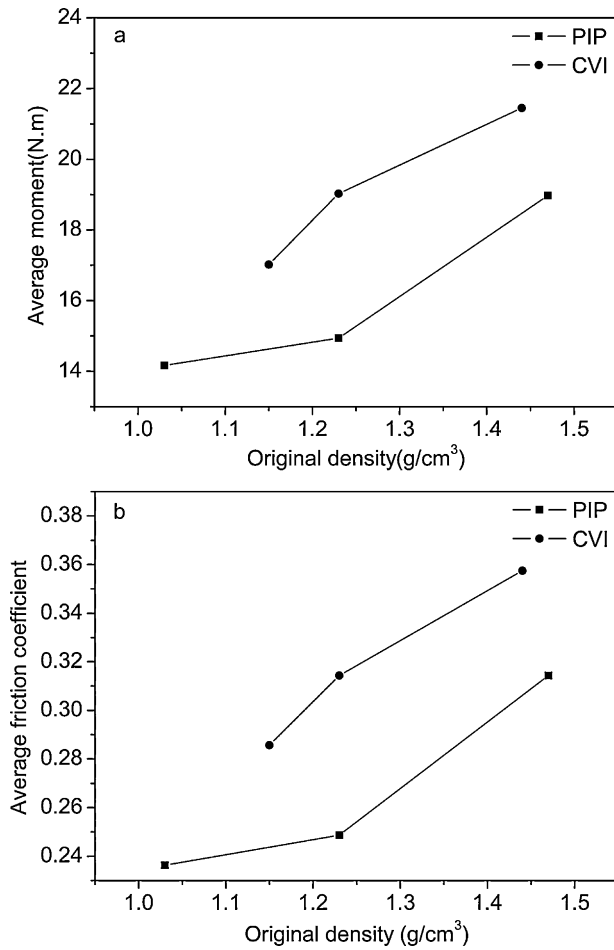


Fig. 5. Average friction coefficient and moment of samples from different methods (a, average moment; b, average friction coefficient).

In addition, Fig. 5 also shows that the average torque and friction coefficient of samples prepared by CVI are a little higher than that by PIP method. For the samples prepared by PIP, concentration grads exist in the procedure of precursor impregnation, thus the pore size and distribution are relatively uneven. The SiC particles in samples prepared by CVI are more

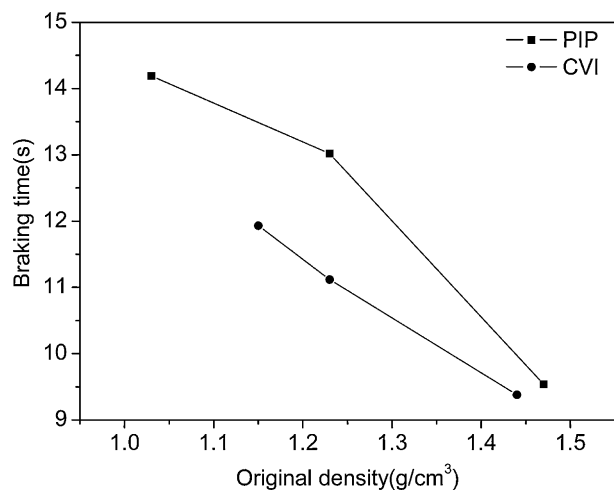


Fig. 6. Braking time of samples from different methods.

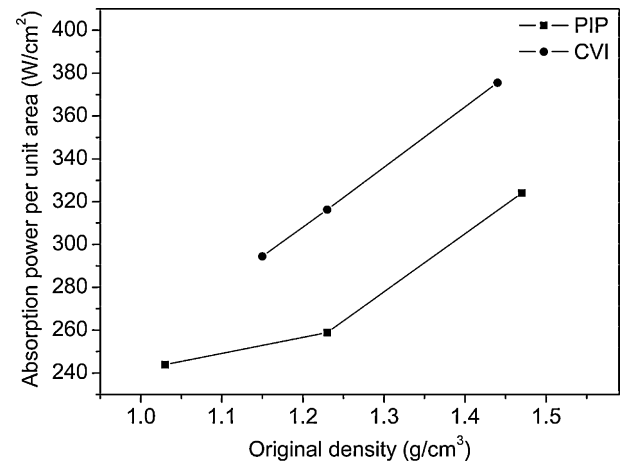


Fig. 7. Absorption power per unit area of samples from different methods.

likely to connect mutually and form the framework, and the friction coefficient of samples from CVI is thus higher than that from PIP.

Fig. 6 shows the braking time of samples from different methods. Because the friction coefficient increases with the increase of the original preform density, the absorption power per unit area also increases significantly (Fig. 7). And moreover, the absorption power unit area of samples from

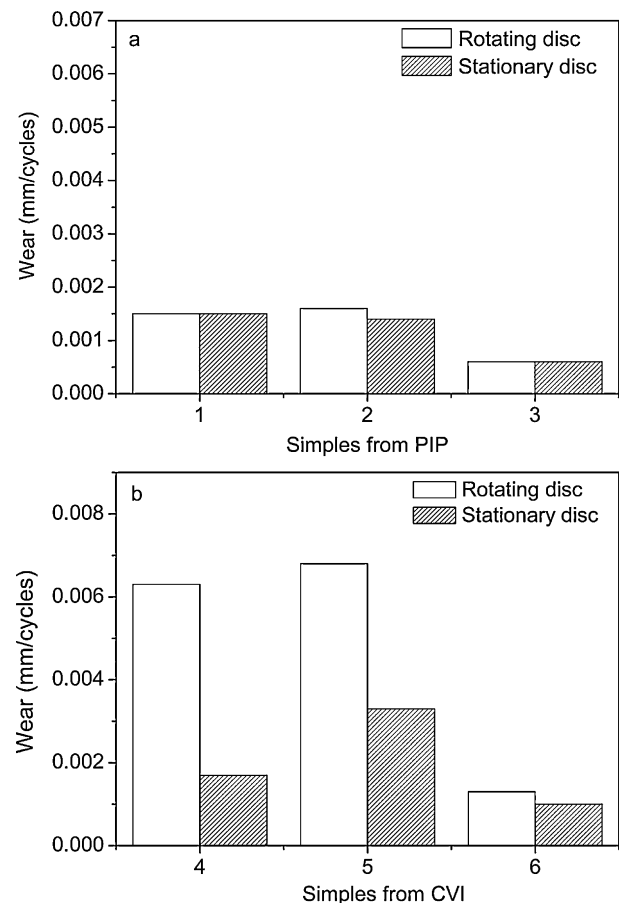


Fig. 8. Wear rate of samples from different methods (a, PIP; b, CVI).

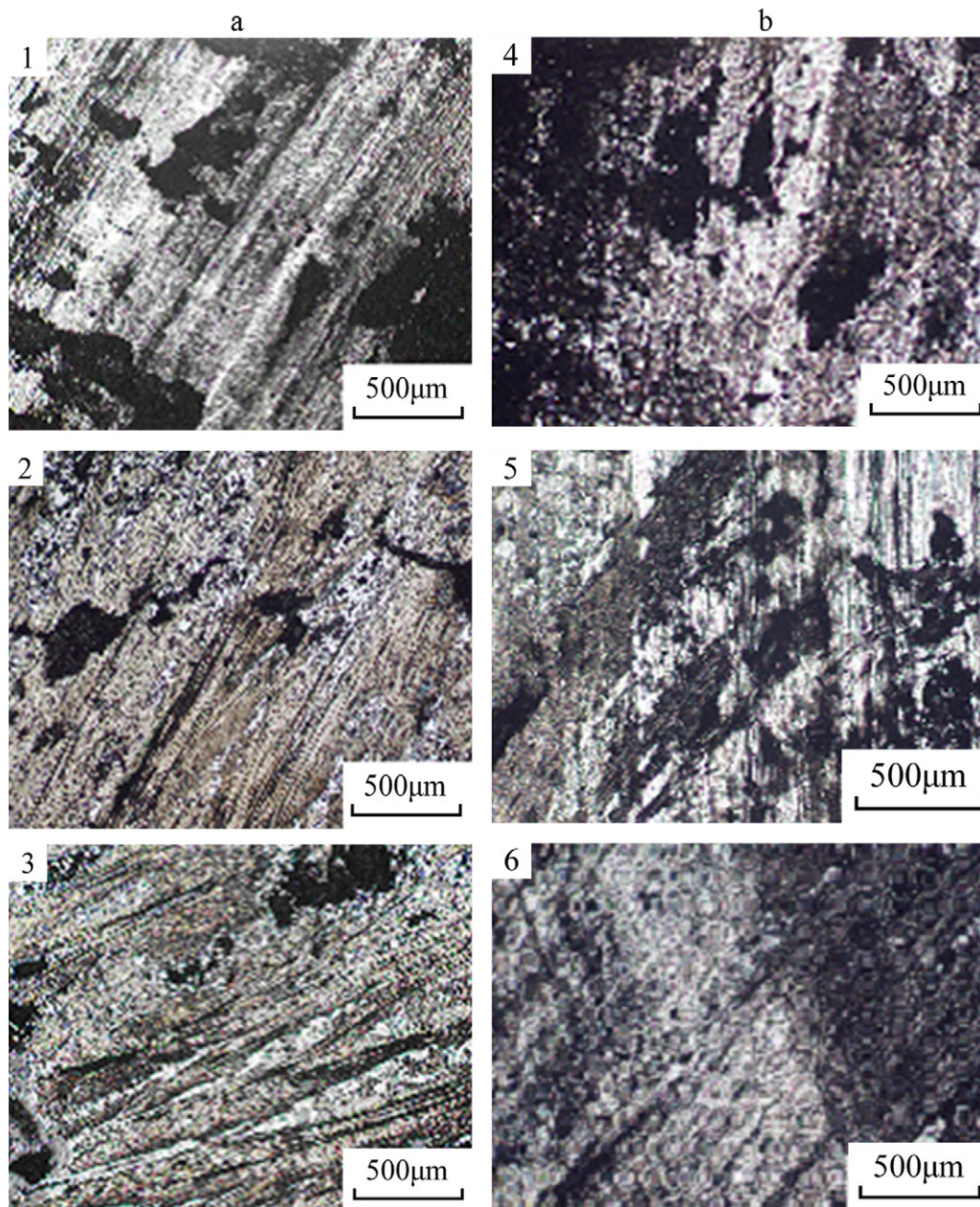


Fig. 9. Micrographs of the friction surface of samples from different methods after braking tests (a, PIP; b, CVI).

CVI is higher than that from PIP, thus the brake time of samples from CVI is much lower than that from PIP.

3.3. Wear properties

Fig. 8 shows the wear rate of samples prepared by different methods. It can be seen that the samples with lower original density possess higher wear rate (Fig. 9), which could be attributed to their higher porosity. For the samples with higher porosity, the SiC particles are not easy to form the framework. A mass of rigid SiC grains act as hard points, plough and micro-cut on the friction surfaces, resulting in the grain-abrasion [13]. Meanwhile, oxidation-abrasion is prone to occur in samples with larger porosity. And local high temperature caused by

grain-abrasion can speed up oxidation-abrasion and fatigue wear. Consequently, evident worn trace could be seen on the surfaces of Groups 1 and 4 from Fig. 9.

Fig. 8 also shows that the wear rate of samples from CVI is higher than that from PIP, which could be attributed to the higher friction coefficient of samples from CVI than that from PIP. The larger the friction coefficient is, the worse the surfaces of samples are damaged.

4. Conclusions

As the original preform densities increasing, the content of SiC and porosity in the obtained composites decreased, which is the key factor influencing the friction and wear properties

greatly. The samples with the largest original density possess the largest friction coefficient, the shortest braking time, and the lowest wear rate. Compared with the samples from PIP, the samples from CVI have a little higher the coefficient, shorter the braking time and higher the wear rate.

Acknowledgements

This work was financed by the National Natural Science Foundation of China (Grant No. 51072165), and the fund of State Key Laboratory of Solidification Processing in Northwestern Polytechnical University (No. KP200901).

References

- [1] G. Savage, Applications of carbon–carbon composites, in: G. Savage (Ed.), *Carbon–Carbon Composites*, 1st ed., Chapman & Hall, London, 1993 pp. 323–346.
- [2] C. Peng, C. Zhijun, L. Shujie, Rapid densification and properties of C/C brake discs, *Acta Mater. Compos. Sin.* 25 (4) (2008) 101–105.
- [3] N.H. Tai, H.H. Kuo, J.H. Chern Lin, et al., Mechanical and tribological properties of 2-D carbon/carbon composites densified through pulse chemical vapor infiltration, *J. Mater. Sci.* 37 (2002) 3693–3703.
- [4] H.H. Kuo, J.H. Chern Lin, C.P. Ju, Effect of a post-treatment on tribological behavior of PAN/CVI and pitch/phenolic/CVI-based C/C composites, *J. Mater. Sci.* 40 (2005) 3263–3265.
- [5] X. Liao, H. Li, W. Xu, et al., Study on the thermal expansion properties of C/C composites, *J. Mater. Sci.* 42 (2007) 3435–3439.
- [6] D. Wang, Y. Liu, Present situation of friction materials, *Adv. Ceram.* 3 (2007) 15–19.
- [7] M. Hokao, S. Hironaka, Y. Suda, et al., Friction and wear properties of graphite/glassy carbon composites, *Wear* 237 (2000) 54–62.
- [8] W. Krenkel, F. Berndt, C/C–SiC Composites for space applications and advanced friction systems, *Mater. Sci. Eng. A* 412 (2005) 177–181.
- [9] P. Xiao, X. Xiong, Y. Ren, Effect and mechanism of different components of C/C–SiC composites on friction and wear behaviors, *Chin. J. Nonferrous Met.* 15 (7) (2005) 1040–1044.
- [10] L. Zhuan, X. Peng, X. Xiang, H. Boyun, Manufacture and properties of carbon fibre-reinforced C/SiC dual matrix composites, *New Carbon Mater.* 25 (3) (2010) 225–231.
- [11] J. Zhang, S. Fan, L. Zhang, et al., Microstructure and frictional properties of 3D needled C/SiC brake materials modified with graphite, *Trans. Nonferrous Met. Soc. China* 20 (2010) 2289–2293.
- [12] P. Xiao, X. Xiong, H. Zhang, et al., Progress and application of C/C–SiC ceramic braking materials, *Chin. J. Nonferrous Met.* 15 (5) (2005) 667–674.
- [13] S. Fan, L. Zhang, L. Cheng, et al., Wear mechanisms of the C/SiC brake materials, *Tribol. Int.* 44 (2011) 25–28.
- [14] Y. Zhang, Y. Xu, J. Lou, et al., The analysis of friction and wear performance of C/C–SiC composites, *J. Aeronaut. Mater.* 25 (2) (2005) 49–54.